METALLURGICAL EVALUATION OF A DOT-3AL2015 CYLINDER

FaAA Project No.: DC17916.000

Prepared for:

U.S. Department of Transportation
400 Seventh Street S.W.
Washington, D.C. 20590

Prepared by:

Timothy R. Smith, Ph.D., P.E.
Failure Analysis Associates, Inc.
310 Montgomery Street
Alexandria, VA 22314

September 1997

TABLE OF CONTENTS

LIST OF FIGURES

1.0 Introduction

The U.S. Department of Transportation (DOT) contracted with Failure Analysis Associates, Inc. (FaAA) to perform a metallurgical examination of the remains of a failed aluminum cylinder. The cylinder was a DOT-3AL2015 type[1] with serial number E5917 manufactured by Luxfer USA and was labeled for use as an oxygen cylinder. The cylinder history was not known to FaAA at the time of this evaluation.

The scope of this investigation was to perform a detailed evaluation of the cylinder remains, including photodocumentation and non-destructive examinations, chemical and mechanical property determination, metallographic sectioning, and fractography. The detailed workscope for this evaluation is provided in Appendix A. This report presents the findings of this evaluation.

2.0 Visual Examination

A visual examination of the cylinder remains was performed. The remains are shown in Figure 1, in the as-received condition. The cylinder broke apart into three large pieces. The remains inspected by FaAA also included some aluminum chips (in the plastic bag shown in Figure 1), presumably from drilled holes at unknown location(s) and a circular sample of material cut from one piece that contained burn markings, presumably from tests by optical emission spectroscopy to determine its bulk chemistry.

The first hydrostatic test on the cylinder was performed in 9/82, based on stampings on the neck. This is taken as its date of manufacture. Additional stampings on the neck and at the base of the cylindrical portion indicate Luxfer USA was the manufacturer. Inspection stampings indicated that the cylinder had been pressure re-tested in 7/88 and 12/93. The 1988 test is followed by a + stamping, which appears to be in error[2]. The bottom of the cylinder has addition stampings of T52 and E903, which are the heat number and cast number, respectively. A complete photodocumentation of the pieces was undertaken and is presented in Appendix B.

The fracture surfaces of the cylinder were inclined (i.e., non-radial with respect to the cylinder axis) shear-type, except for a portion of the sidewall where the fracture surfaces were flat and radial with respect to the axis of the cylinder. In the neck region, the fracture did not pass through a diameter of the inlet hole.

3.0 Quantitative Chemical Analysis

A portion of the cylinder was removed and tested by optical emission spectrometry to determine the chemical composition. The results of this analysis are shown in Table 1

[1] This cylinder is intended to satisfy the requirements of the DOT-3Al section of 49 CFR-178.46.
[2] The "+" stamping is indicative of a 10% overfill pressure (i.e., a fill of 110% of the rated pressure) for steel cylinders and is not applicable to DOT-3Al cylinders.

and indicate that the cylinder conforms to the Aluminum Association (AA) 6351 alloy specification and satisfies the DOT-49 CFR-178.46 specification for aluminum alloy chemistry.

Table 1: Chemistry of the Cylinder, Neck Region

Element	Composition (wt.%)		
	Test Result	AA6351 Specification (low)	AA6351 Specification (high)
Mg	**0.74**	**0.40**	**0.80**
Si	**1.02**	**0.70**	**1.30**
Ti	**0.04**	**0.00**	**0.20**
Mn	**0.52**	**0.40**	**0.80**
Fe	**0.24**	**0.00**	**0.50**
Cu	**0.02**	**0.00**	**0.10**
Zn	**0.03**	**0.00**	**0.20**
OE	**<0.05**	**0.00**	**0.05**
OT	**<0.15**	**0.00**	**0.15**
Al	**Balance**	**balance**	**balance**

Chemical composition determined by optical emission spectrometry in accordance with the ASTM-E1019-91 standard. "OE" denotes "other elements", "OT" denotes the total of all "other elements" not listed in the table.

Chip samples were taken using an electric drill from the neck, the sidewall, and the bottom of the cylinder. These chips were dissolved in solution and analyzed by atomic absorption spectrometry to determine their chemical composition, Table 2.

Table 2: Chemistry of the Cylinder

Element	Composition (wt.%)				
	Test Result Neck	Test Result Sidewall	Test Result Bottom	49 CFR-178.46-5 Specification (low)	49 CFR-178.46-5 Specification (high)
Mg	**0.71**	**0.70**	**0.69**	**0.40**	**0.80**
Si	**0.80**	**0.80**	**0.80**	**0.70**	**1.30**
Ti	**0.04**	**0.04**	**0.04**	**0.00**	**0.20**
Mn	**0.53**	**0.56**	**0.55**	**0.40**	**0.80**
Fe	**0.22**	**0.22**	**0.22**	**0.00**	**0.50**
Cu	**0.09**	**0.06**	**0.05**	**0.00**	**0.10**
Zn	**0.02**	**0.02**	**0.02**	**0.00**	**0.20**
Bi	**<0.0050**	**<0.0050**	**<0.0050**	**0.00**	**0.01**
Pb	**0.0060**	**0.0090**	**0.0130**	**0.00**	**0.01**
Al	**Balance**	**Balance**	**balance**	**balance**	**Balance**

Chemical composition determined by atomic absorption spectrometry in accordance with the ASTM-E663 and ASTM-D3335 standards.

These results show compliance with the DOT federal regulation 49 CFR 178.46-5 valid at the time of the cylinder's manufacture. The chemistry is also in compliance with the current DOT federal regulation 49 CFR 178.46-5, except for the Pb level in the bottom of

the tank which was above the current limit[3] of 100 weight-ppm (13 atomic-ppm[4]). No significant variations based on the sample location from within the cylinder were found for any other element tested for. Note that the Bi levels were below 50 weight-ppm (6.5 atomic-ppm), which is the detection limit of the technique used.

4.0 Mechanical Testing

4.1 Tensile Testing

Tensile tests were performed at room temperature on standard size ASTM A370 tensile test coupons from the cylinder wall, aligned along the cylinder axis. Sectioning was performed on fragment 1A-1, Figure 4. Component 1A-1F was used for the tensile test coupons, as it contained material minimally deformed by the cylinder rupture. Three full-thickness coupons were machined and Figure 4b shows them in the post-tested configuration. The test data are shown in Table 3.

The average values found are above the current 49 CFR 178.46-5 minimum specification. They compare well with values of 42.8 ksi yield strength, 49.3 ksi ultimate strength and 13% elongation (2 inch gauge length), published for 6351 in T6 temper [1]. DOT CFR 49 178.46-5 requires that the material be AA6351-T6.

Table 3: Mechanical Properties

Test	Yield (ksi)	UTS (ksi)	Elongation (%)	49 CFR 178.46-5 Yield (min.) (ksi)	49 CFR 178.46-5 UTS (min.) (ksi)	Elongation (%)
1A-1F#1	**43.9**	**50.5**	**17.0**	**37.0**	**42.0**	**14**
1A-1F#2	**42.4**	**50.5**	**17.0**	**37.0**	**42.0**	**14**
1A-1F#3	**42.4**	**50.5**	**16.0**	**37.0**	**42.0**	**14**
Average	**42.9**	**50.5**	**16.7**	**37.0**	**42.0**	**14**

Notes:

1. Tests were performed in accordance with the ASTM A370-77 Standard; gauge length was 2 inches.
2. *Yield denotes the yield strength (0.2% offset), UTS denotes ultimate tensile strength.*
3. Elongation values from the flat coupons tested here differ from the 49 CFR 178.46-5 values based on cylindrical specimens.

4.2 Hardness Testing

Rockwell hardness measurements were made on a slice removed from the tank sidewall area of fragment 1A-1B (see Figure 4). A total of five measurements were taken; the results are shown in Table 4.

[3] Note that the upper limit for Pb was reduced from 500 wt-ppm to 100 wt-ppm in the 1988 edition of 49 CFR 178.46-5.

[4] calculated using the equation: atomic-ppm (Pb) = weight-ppm (Pb)*GMW(Al)/GMW(Pb); where GMW is the gram molecular weight of the element in parenthesis. The same equation was used for the bismuth level with Bi replacing Pb.

Table 4: Hardness Measurements

Component	Indent No.	Hardness (Rockwell B)	Average Hardness (Rockwell B)
1A-1B	1	47.8	50.4 HRB
	2	48.0	
	3	48.7	
	4	52.7	
	5	54.8	

Rockwell hardness measurements were made using a 100 kg load on a Leco RT-370 hardness tester.

5.0 Sectioning and Metallography

The fracture surface in the neck region on one side of the inlet hole (marked "A" in Figure 3) was sliced on a plane that was approximately parallel to the fracture surface. This portion was chosen for detailed fractographic examination (see below) as it appeared to be representative of the fracture surface in the neck region.

Sections were cut from the sidewall region, Figure 5, for metallography, hardness testing, and to remove a portion of the fracture surface (see Figure 1) for further detailed examination. The section for metallography (MET) was polished and etched using standard techniques and photographed under polarized light to reveal the grain structure, Figure 6. Note that, in these micrographs, the grain boundaries are lighter than the matrix. The microstructure observed appears to be typical for AA6351-T6 [2].

6.0 Fractography

Figure 7 shows detailed optical and scanning electron microscope (SEM) fractographs of the fracture surface "A" from the neck region. Note that the fracture surface in this region is not planar and is non-radial with respect to the cylinder axis. Three regions of the fracture surface were studied in detail, labeled in Figure 7a. Region 1 is at the inside surface close to the inlet hole threads. This region shows a mixture of intergranular and transgranular fracture, with very fine-scale dimples on the facets. Figure 7b shows that this region is roughly parallel to the cylinder axis. At the inside surface, the fracture continues parallel to the axis for a short distance, and then moves off onto other planes. The Region 1 area is consistent, in morphology and extent, with a shallow crack at one of the folds present at the inside wall of the cylinder (see Figures 2a and 3). These folds were formed during the cylinder's manufacture.

Region 2, further up the inlet hole, and Region 3, near to the outside surface of the cylinder, are not coplanar with Region 1. Both show ductile dimpled rupture as a failure mode. This is the predominant failure mode for most of the neck region.

Figure 8 shows energy dispersive spectra (EDS) captured from Region 1 and Region 2. These spectra show surface chemistry and the expected peaks for aluminum (Al), manganese (Mn), and iron (Fe) (compare with Tables 1 and 2).

The fracture surface in the sidewall region identified in Figure 1 was studied in detail. Figure 9 shows close-up photograph montages of the fracture surface and a view of the exterior surface of the cylinder at this location. The fracture surface contains several discoloration marks, Figure 9a. In this region, the sidewall fracture is flat and radial with respect to the cylinder axis and runs longitudinally parallel to the cylinder axis. The fracture in this area runs along a series of indentation marks (i.e., mechanical damage) on the exterior surface of the cylinder, Figure 9b. This damage was more extensive on the exterior surface than in depth, and penetrated typically less than 10% of the wall thickness. At both ends of the region containing the discoloration, the fracture surface changes to a slant-type (i.e., non-radial with respect to the cylinder axis) morphology.

Figure 10 shows an scanning electron image montage of the sidewall fracture shown in Figure 9. The flat, discolored regions correspond to regions of intergranular fracture. Some of these regions show microdimpling on the grain facets. Varying degrees of oxidation/corrosion are also seen on these facets. The intergranular facets should be compared with the microstructure of the sidewall region shown in Figure 6. The intergranular flat regions form a feature of approximately 2 inches in length axially, and penetrating about 90% of the wall thickness from the exterior. The thin band (i.e., approximately 10% of the wall thickness) near to the inside surface is characterized by ductile dimpled rupture. The slant-type regions at both ends of the flat area are characterized by ductile dimpled rupture, with some faceting.

An EDS spectrum was acquired from one of the intergranular fracture regions (i.e., Region 1,2 in Figure 10). An SEM micrograph of this region and the EDS spectrum are shown in Figure 11. The peaks of aluminum (Al), manganese (Mn), iron (Fe) and silicon (Si) all correspond to alloy constituents (compare with Tables 1 and 2). Oxidation/corrosion products are indicated by the presence of oxygen (O), sulfur (S), potassium (K) and chlorine (Cl). Comparing Figure 11 with the intergranular fracture regions shown in Figure 10 indicate that varying degrees of oxygen/corrosion occurred in these regions. This finding suggests that the intergranular region formed before the dimpled rupture regions developed.

Figure 12 shows SEM fractographs of the fracture surface from one of the tensile specimens (specimen 1A-1F1A, Figure 4) used for mechanical property determination. Note that the fracture surface is primarily ductile dimpled rupture, with both macro and micro dimples, and some intergranular faceting, with microdimpling on these facets. This morphology is consistent with fractographic studies of similar Al alloys in tensile and toughness testing [4]. A comparison of Figure 12 with the dimpled rupture regions of Figures 7 and 10, suggests that those regions are likely attributable to overload.

7.0 Discussion

Examination and testing of the cylinder remains demonstrates that the subject cylinder meets the chemical and mechanical property requirements of the DOT 49 CFR 178.46 in force at the time of manufacture. The cylinder's chemistry also meets the requirements of the current 49 CFR 178.46-5 for all elements except the lead (Pb) level which is exceeded in the bottom of the cylinder only. The composition of the alloy indicates that it complies with the Aluminum Association specification for AA6351-T6 in accordance with 49 CFR 178.46-5. The microstructure appears to be typical for this alloy and heat treatment.

Examination of the fracture surfaces of the cylinder suggests that the fracture did not originate in the neck region[5], either associated with the neck threads or any cracks that formed from manufacturing folds in the inside surface. Fractography suggests that a small crack from one of the folds existed in the neck region and was incorporated into the fracture surface. The slant-type morphology and the predominantly dimpled rupture failure mode in most of the neck region suggest that the neck area was in the crack propagation path and that the fracture originated from elsewhere in the cylinder.

Examination of the fracture surfaces of the largest fragment strongly suggests that the failure originated from the sidewall region of the cylinder at a location with mechanical damage on the exterior surface. This damage, in the form of a longitudinal series of plastic indentation marks in the exterior cylinder surface, appear to have initiated multiple regions of intergranular corrosive attack. The presence of this corrosion here and not elsewhere on the fracture surface indicates that this feature predated the time of the cylinder's rupture. It is known that excess-silicon aluminum alloys like AA6351 can be susceptible to intergranular corrosion in the T6 temper [3]. This attack may have been assisted by small cracks or residual stresses in the cylinder wall associated with the plastic deformation. The intergranular regions appear to have linked up to form a contiguous crack, of approximately 2 inches in length axially, and penetrating about 90% of the wall thickness from the exterior. Failure of the tank resulted from the unstable propagation of this sidewall crack.

[5] Earlier work by J. H. Smith [5] indicates that cracking in the neck region has been reported in other similar cylinders.

8.0 Summary and Conclusions

A metallurgical examination of an aluminum cylinder DOT-3AL2015 type, with serial number E5917 showed the following results.

- This 1982-vintage cylinder meets the chemical specifications of the 49 CFR 178.46-5 for AA6351 alloy in force at the time of manufacture. The cylinder also meets the current 49 CFR 178.46-5 specification for all elements except lead (Pb), as measured at the bottom of the cylinder only.

- This 1982-vintage cylinder meets the mechanical property specifications of the 49 CFR 178.46-5 and 178.46-13 (both at the time of manufacture and the current edition).

- The cylinder failure initiated from the sidewall near to a series of surface indentation marks attributable to mechanical damage. Multiple sites of intergranular corrosive attack beneath these indentation marks (pre-dating the cylinder's rupture) apparently linked to form a crack approximately 2 inches in length and penetrating about 90% of the wall thickness from the exterior. This crack then propagated unstably to failure.

- Fracture did not initiate in the neck region. A small (inner surface) crack was found fractographically in the neck region which was incorporated into the running fracture (i.e., fracture did not originate from this crack). Multiple small folds in the interior wall in the neck region near the inlet hole were found associated with the cylinder's manufacture, but do not appear to be the initiating fracture locations.

- Fracture was not associated with the neck threads.

9.0 References

1. J. E. Hatch, Ed., (1984). Aluminum: Properties and Physical Metallurgy, American Society for Metals, Metals Park, OH, p. 363.
2. ASM Metals Handbook, 9th. Ed., Vol. 9, "Metallography and Microstructures", American Society for Metals, Metals Park, OH, p. 367.
3. J. E. Hatch, Ed., (1984). Aluminum: Properties and Physical Metallurgy, American Society for Metals, Metals Park, OH, p. 269.
4. M. Guttmann, B. Quantin, and Ph. Dumoulin (1983). "Intergranular creep embrittlement by non-soluble impurity: Pb precipitation hardened Al-Mg-Si alloys", Metal Sci., Vol. 17, No. 3, pp. 123-140.
5. J. H. Smith (1987). "Evaluation of Cracking in Aluminum Cylinders", NBSIR 86-3492, Institute for Materials Science and Engineering, National Bureau of Standards (NBS), U.S. Dept. of Commerce, Gaithersburg, MD.

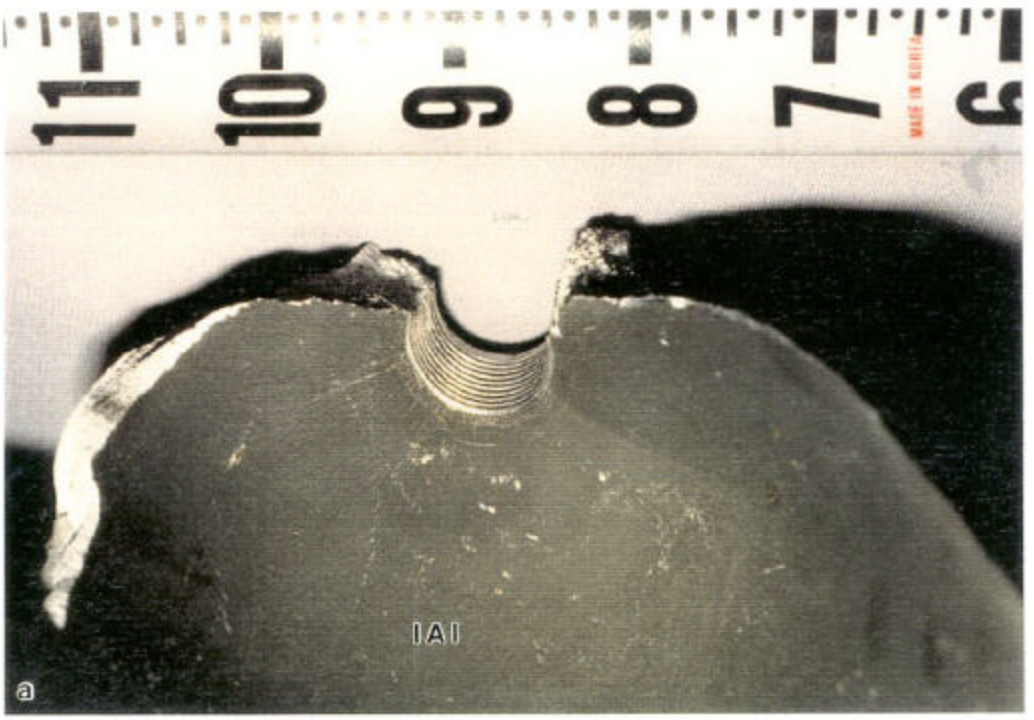

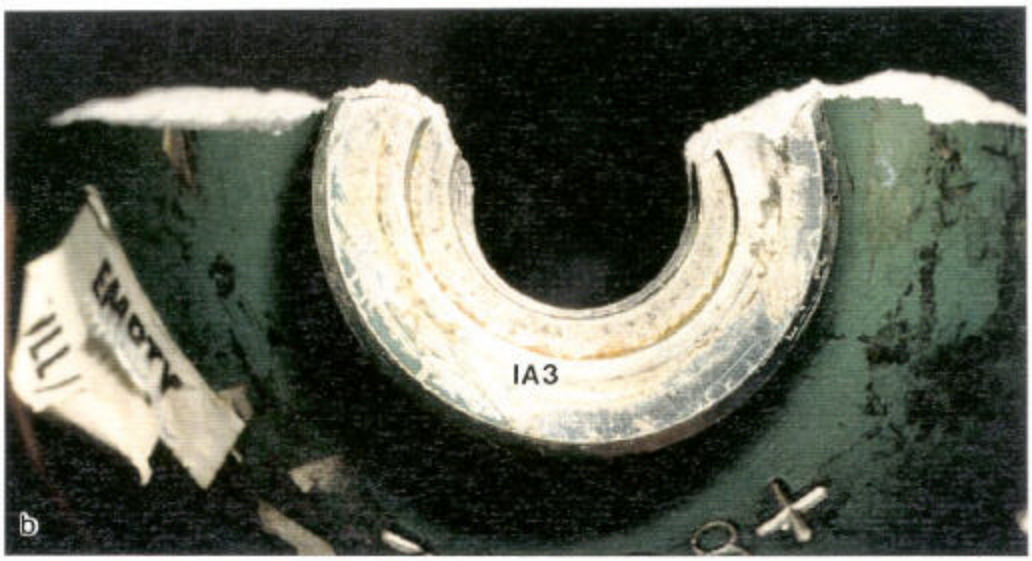

Figure 2. Neck region of failed cylinder.
(a) View inside looking out. Photo ID: DC17916-R2E12.
(b) View looking down on the inlet hole. Photo ID: DC17916-R2E20.

Note that the fracture surface in the neck region is not parallel to the cylinder axis and the fracture path does not pass through a diameter of the inlet hole.

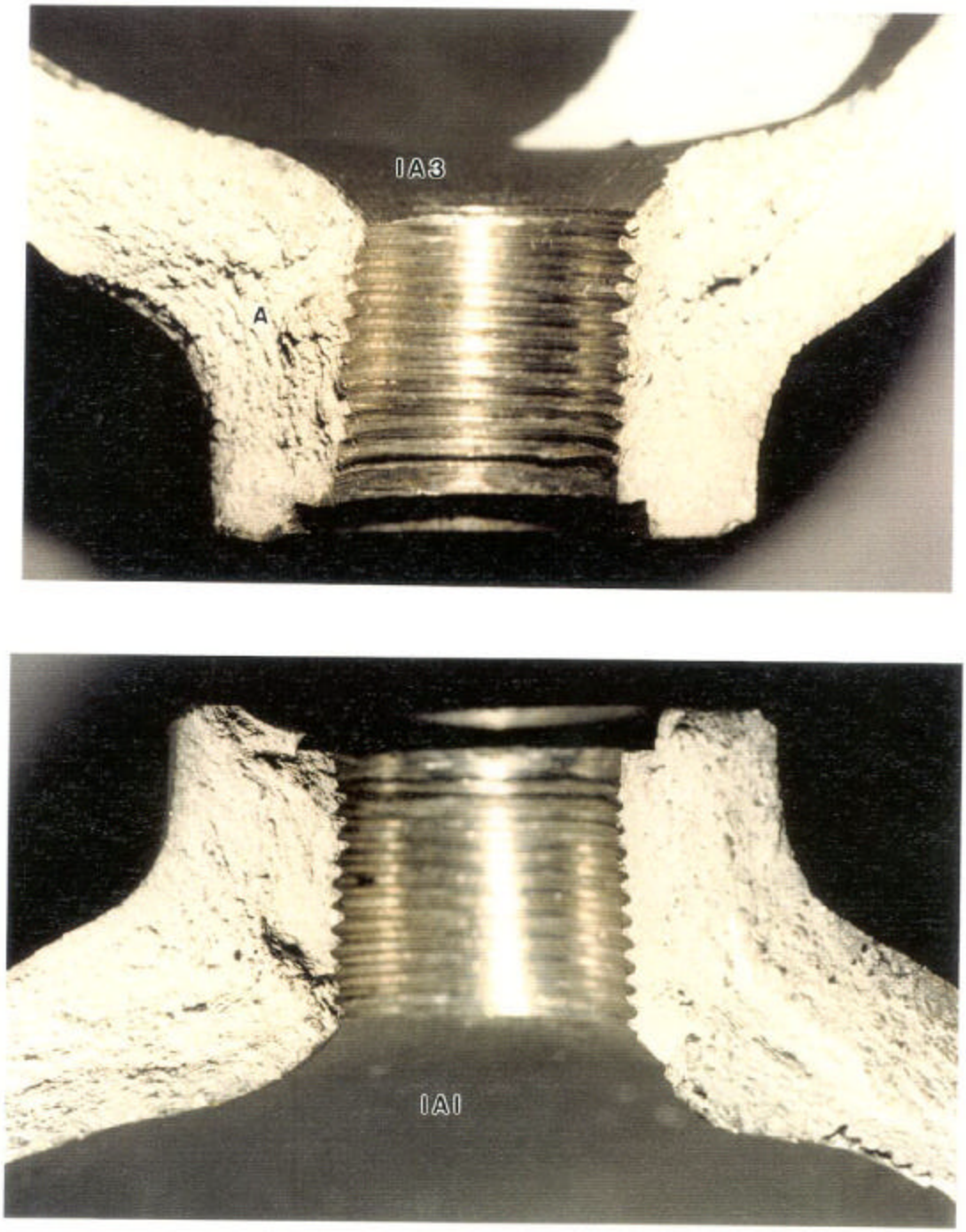

Figure 3. Mating fracture surfaces at the inlet hole.
Fracture surface marked "A" was selected for further study.
Photo ID: DC17916-R3E1 and –R2E15.

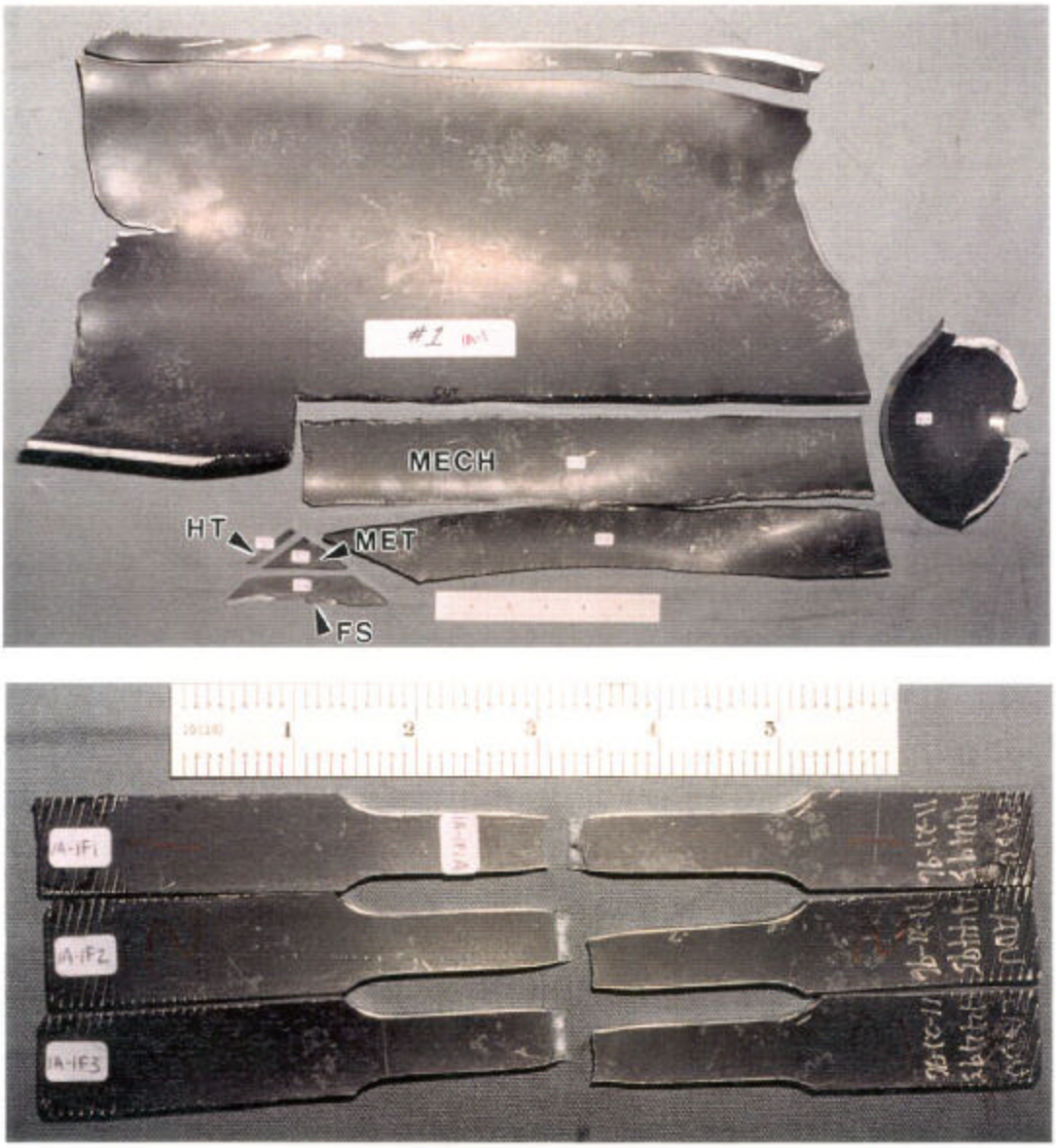

Figure 4. Cylinder fragment 1A-1.

(a) Sections cut. Photo ID: DC17916-R11E19.
Note "MECH" denotes the piece used for machining tensile test coupons, "MET" denotes the section used for metallographic examination, "HT" denotes the section used for Rockwell hardness measurements, and "FS" denotes the fracture surface from the region marked with the arrow in Figure 1.

(b) Tensile test coupons in the post-test condition.
Photo ID: DC17916-R11E20.

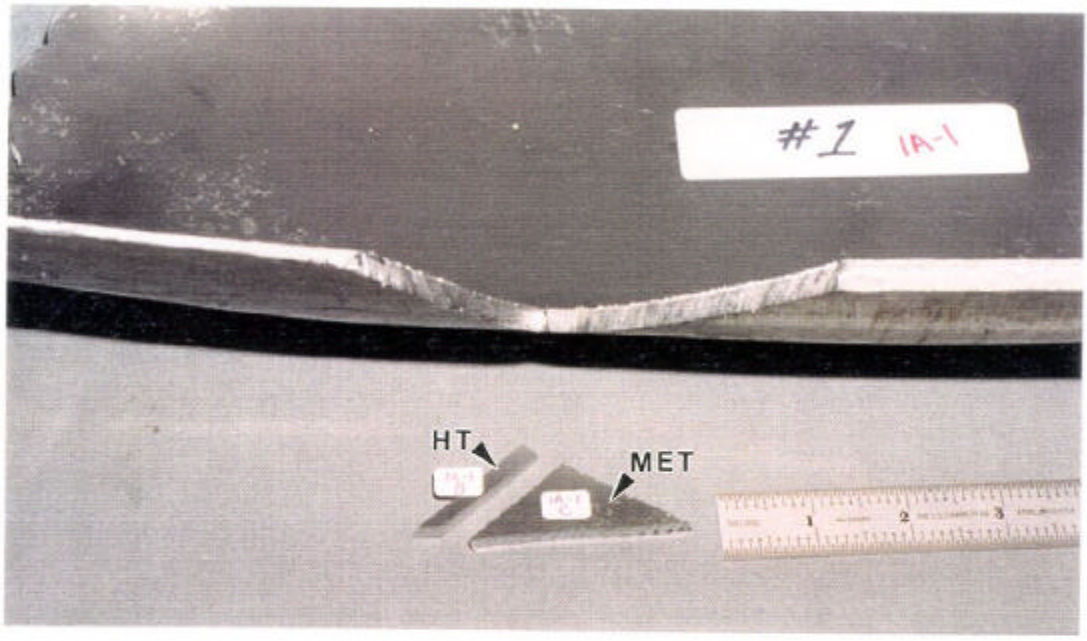

Figure 5. **Close up of sidewall region showing "HT" and "MET" sections from Figure 4.**
Photo ID: DC17916-R11E7.